## Unifying microscopic and continuum treatments of van der Waals and Casimir interactions

Prashanth S. Venkataram, <sup>1</sup> Jan Hermann, <sup>2</sup> Alexandre Tkatchenko, <sup>2,3</sup> and Alejandro W. Rodriguez<sup>1</sup>

We present an approach for computing long-range van der Waals (vdW) interactions between complex molecular systems and arbitrarily shaped macroscopic bodies, melding atomistic treatments of electronic fluctuations based on density functional theory in the former, with continuum descriptions of strongly shape-dependent electromagnetic fields in the latter, thus capturing many-body and multiple scattering effects to all orders. Such a theory is especially important when considering vdW interactions at mesoscopic scales, i.e. between molecules and structured surfaces with features on the scale of molecular sizes, in which case the finite sizes, complex shapes, and resulting nonlocal electronic excitations of molecules are strongly influenced by electromagnetic retardation and wave effects that depend crucially on the shapes of surrounding macroscopic bodies. We show that these effects together can modify vdW interactions by orders of magnitude compared to previous treatments based on Casimir–Polder or non-retarded approximations, which are valid only at macroscopically large or atomic-scale separations, respectively.

Van der Waals (vdW) interactions play an essential role in non-covalent phenomena throughout biology, chemistry, and condensed-matter physics [1–3]. It has long been known that vdW interactions among a system of polarizable atoms are not pairwise-additive but instead strongly depend on geometric and material properties [2, 4, 5]. However, only recently developed theoretical methods have made it possible to account for short-range quantum interactions in addition to longrange many-body screening in molecular ensembles [3, 6-15], demonstrating that nonlocal many-body effects cannot be captured by simple, pairwise-additive descriptions; these calculations typically neglect electromagnetic retardation effects in molecular systems. Simultaneously, recent theoretical and experimental work has characterized dipolar Casimir— Polder interactions between macroscopic metallic or dielectric objects and atoms, molecules, or Bose-Einstein condensates, further extending to nonzero temperatures, dynamical situations, and fluctuations in excited states (as in so-called Rydberg atoms) [16–25]. Yet, while theoretical treatments have thus far accounted for the full electrodynamic response of macroscopic bodies (including retardation), they often treat molecules as point dipoles of some effective bulk permittivities or as collections of noninteracting atomic dipoles, ignoring finite size and other many-body electromagnetic effects.

In this paper, motivated by the aforementioned theoretical developments [1, 16–18, 24–28], we describe an approach that seamlessly connects atomistic descriptions of large molecules to continuum descriptions of *arbitrary* macroscopic bodies, characterizing their mutual vdW interactions. In particular, while molecules that are very close to macroscopic objects require atomistic descriptions of the latter, and very large molecules that are far from macroscopic objects require consideration of the contributions of vibrational (in addition to electronic) resonances to the vdW interaction energy, we focus on a mesoscopic regime involving molecular sizes and separations on the order of 1–100 nm, where macroscopic objects can be treated continuously for the purposes of comput-

ing electromagnetic field responses (and molecular vibrational resonances can be neglected), yet electromagnetic retardation in conjunction with the finite sizes, nontrivial shapes, and non-local electronic correlations of large molecules need to be self-consistently considered to accurately characterize vdW interactions. We specifically investigate interactions among various large molecules and gold surfaces, and show that the effect of nonlocal polarization correlations, encapsulated in the ratio of retarded, many-body (RMB) to pairwise vdW energies (or forces), causes relative deviations from pairwise treatments ranging from 20% to over 3 orders of magnitude; further differences of over an order of magnitude are observed when retardation or finite size effects are neglected.

The basis of our work is an equation for the long-range dispersive vdW energy of a system of polarizable bodies, consisting of N microscopic bodies (molecules), labeled by k and described by electric susceptibilities  $\mathbb{V}_k$ , and a collection of continuum bodies (an environment) described by a collective, macroscopic susceptibility  $\mathbb{V}_{\text{env}}$ , displayed schematically in Fig. 1. The energy of such a collection of bodies can be obtained from the scattering framework [29] and written as an integral over imaginary frequency  $\omega = \mathrm{i}\xi$ ,

$$\mathcal{E} = \frac{\hbar}{2\pi} \int_0^\infty d\xi \, \ln[\det(\mathbb{T}_\infty \mathbb{T}^{-1})], \tag{1}$$

in terms of T-operators that depend on the bodies' susceptibilities as well as on the homogeneous electric Green's function  $\mathbb{G}_0(\mathrm{i}\xi,\mathbf{x},\mathbf{x}') = (\nabla\otimes\nabla-\frac{\xi^2}{c^2}\mathbb{I})\frac{e^{-\frac{\xi|\mathbf{x}-\mathbf{x}'|}{c}}}{4\pi|\mathbf{x}-\mathbf{x}'|} \text{ (including retardation) mediating electromagnetic interactions; they encode the scattering properties of the various bodies, and are given by,$ 

$$\mathbb{T} = \left(\mathbb{I} - (\mathbb{V} + \mathbb{V}_{\mathrm{env}})\mathbb{G}_0\right)^{-1}(\mathbb{V} + \mathbb{V}_{\mathrm{env}}),$$

where  $\mathbb{V} = \sum_k \mathbb{V}_k$ ;  $\mathbb{T}_{\infty} = \mathbb{T}_{\text{env}} \prod_k \mathbb{T}_k$ , written in terms of  $\mathbb{T}_{k(\text{env})} = (\mathbb{I} - \mathbb{V}_{k(\text{env})} \mathbb{G}_0)^{-1} \mathbb{V}_{k(\text{env})}$ , encodes the scattering response of the bodies in isolation from one another [29].

The energy in (1) treats microscopic and macroscopic bodies on an equal footing, yet the key to its accurate evalua-

<sup>&</sup>lt;sup>1</sup>Department of Electrical Engineering, Princeton University, Princeton, New Jersey 08544, USA

<sup>&</sup>lt;sup>2</sup>Fritz-Haber-Institut der Max-Planck-Gesellschaft, Faradayweg 4–6, 14195, Berlin, Germany

<sup>&</sup>lt;sup>3</sup>Physics and Materials Science Research Unit, University of Luxembourg, L-1511 Luxembourg (Dated: August 6, 2021)

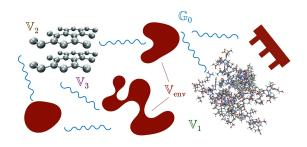


Figure 1. Schematic of molecular bodies described by electric susceptibilities  $\mathbb{V}_n$  in the vicinity of and interacting with macroscopic bodies described by a collective susceptibility  $\mathbb{V}_{\text{env}}$ , where the interactions are mediated by vacuum electromagnetic fields  $\mathbb{G}_0$ .

tion lies in appropriately representing the degrees of freedom (DOFs) of each entity. Typically, macroscopic environments are well described by continuum susceptibilities  $V_{\rm env}$ , whose response can be expanded in a basis of incoming and outgoing propagating planewaves, as is typical of the scattering framework [29], or via localized functions, e.g. tetrahedral mesh elements, in brute-force formulations [27, 30]. Microscopic bodies, on the other hand, generally require quantum descriptions, but recent work has shown that one can accurately represent their response  $\mathbb{V}_k = \sum_p \alpha_p |f_p\rangle \langle f_p|$  through bases  $\{|f_p\rangle\}$  of either exponentially localized (for insulators) or polynomially delocalized (for metals) functions [31], that accurately capture multipolar interactions among electronic wavefunctions [3, 6, 8, 13]. For molecules with finite electronic gaps, the bare response is well described by sums over dipolar ground-state oscillator densities [5, 8–10, 12, 14, 32],

$$f_p(i\xi, \mathbf{x}) = \left(\sqrt{2\pi}\sigma_p(i\xi)\right)^{-3} \exp\left(-\frac{(\mathbf{x} - \mathbf{x}_p)^2}{2\sigma_p^2(i\xi)}\right),$$
 (2)

centered at the locations  $\mathbf{x}_p$  of each atom p, normalized such that  $\int \mathrm{d}^3\mathbf{x} \, f_p = 1$ , and featuring a Gaussian width that, rather than being phenomenological [33, 34], depends on the atomic polarizability via  $\sigma_p(\mathrm{i}\xi) = \left(\frac{\alpha_p(\mathrm{i}\xi)}{\sqrt{72\pi^3}}\right)^{1/3}$  [8, 35]. The isotropic atomic polarizabilities  $\alpha_p$  are computed via density functional theory, as in recent works [8, 9], which include short-range electrostatic, hybridization, and quantum exchange effects.

Since microscopic and macroscopic bodies are assumed to be disjoint, it is more efficient to partition the T-operators into blocks belonging to either molecules or macroscopic objects, allowing a trace over the macroscopic DOFs. The definitions of  $\mathbb{T}_{k(\text{env})}$  imply  $\mathbb{T}_{k(\text{env})}^{-1}=\mathbb{V}_{k(\text{env})}^{-1}-\mathbb{G}_0$ , which means that the relevant T-operators can be written as:

$$\mathbb{T}^{-1} = \begin{bmatrix} \mathbb{T}_{\text{mol}}^{-1} & -\mathbb{G}_0 \\ -\mathbb{G}_0 & \mathbb{T}_{\text{env}}^{-1} \end{bmatrix}, \quad \mathbb{T}_{\infty} = \begin{bmatrix} \mathbb{T}_{\text{mol},\infty} & 0 \\ 0 & \mathbb{T}_{\text{env}} \end{bmatrix}$$
(3)

thus partitioning the molecular and macroscopic (environmen-

tal) DOFs. These depend on the molecular T-operators

$$\mathbb{T}_{\text{mol}}^{-1} = \begin{bmatrix}
\mathbb{T}_{1}^{-1} & -\mathbb{G}_{0} & \dots & -\mathbb{G}_{0} \\
-\mathbb{G}_{0} & \mathbb{T}_{2}^{-1} & \dots & -\mathbb{G}_{0} \\
\vdots & \vdots & \ddots & \vdots \\
-\mathbb{G}_{0} & -\mathbb{G}_{0} & \dots & \mathbb{T}_{N}^{-1},
\end{bmatrix}$$
(4)

with  $\mathbb{T}_{\text{mol},\infty} = \prod_k \mathbb{T}_k$ , which are in turn partitioned into blocks for each of the N molecular bodies. Given this, the product in the determinant can be evaluated as:

$$\begin{split} \det(\mathbb{T}_{\infty}\mathbb{T}^{-1}) &= \det(\mathbb{T}_{\mathrm{mol},\infty}\mathbb{T}_{\mathrm{mol}}^{-1}) \det(\mathbb{I} - \mathbb{G}_{0}\mathbb{T}_{\mathrm{env}}\mathbb{G}_{0}\mathbb{T}_{\mathrm{mol}}) \\ &= \det(\mathbb{T}_{\mathrm{mol},\infty}\mathbb{T}_{\mathrm{mol}}^{-1}) \det(\mathbb{I} - \mathbb{G}_{\mathrm{env}}\mathbb{V}) \\ &\quad \times \det(\mathbb{I} - \mathbb{G}_{0}\mathbb{V})^{-1} \end{split} \tag{5}$$

where we used the property  $\mathbb{G}_0\mathbb{T}_{k(\mathrm{env})}=(\mathbb{I}-\mathbb{G}_0\mathbb{V}_{k(\mathrm{env})})^{-1}-\mathbb{I}$ , and consolidated the scattering properties of the macroscopic bodies into the operator  $\mathbb{G}_{\mathrm{env}}=\mathbb{G}_0(\mathbb{I}-\mathbb{V}_{\mathrm{env}}\mathbb{G}_0)^{-1}$ , which solves

$$\left[\nabla \times \nabla \times + \frac{\xi^2}{c^2} \left( \mathbb{I} + \mathbb{V}_{\text{env}} \right) \right] \mathbb{G}_{\text{env}} = -\frac{\xi^2}{c^2} \mathbb{I}$$
 (6)

for an imaginary frequency  $\omega=\mathrm{i}\xi$ , thereby encoding the macroscopic DOFs purely in the electric field response; this can be solved via any number of state-of-the-art analytical or numerical classical electrodynamic techniques [1, 26–28], including but not limited to scattering [29, 30, 36] and finite-difference [37–39] methods. Moreover, as the molecules are all disjoint, then  $\det(\mathbb{T}_{\mathrm{mol},\infty}\mathbb{T}_{\mathrm{mol}}^{-1}) = \det(\mathbb{I} - \mathbb{G}_0\mathbb{V})\prod_k \det(\mathbb{I} - \mathbb{G}_0\mathbb{V}_k)^{-1}$ . Putting all of these identities together yields the following expression for the energy:

$$\mathcal{E} = \frac{\hbar}{2\pi} \int_0^\infty d\xi \, \ln[\det\left(\mathbb{M}\mathbb{M}_{\infty}^{-1}\right)] \tag{7}$$

where 
$$\mathbb{M} = \mathbb{I} - \mathbb{G}_{env} \mathbb{V}$$
 and  $\mathbb{M}_{\infty} = \prod_{k} (\mathbb{I} - \mathbb{G}_0 \mathbb{V}_k)$ .

The above log-determinant formula for the energy includes retardation by construction and accounts for manybody screening and multiple scattering to all orders, thereby ensuring full consideration of finite size, complex shape effects, and collective polarization excitations (see supplement for an alternate equivalent derivation including all of these effects). Moreover, existing sophisticated techniques for modeling molecular and electromagnetic-field responses come together in the operator products  $\mathbb{GV}_k$ ; when represented in the p-dimensional molecular basis  $\{|f_p\rangle\}$ , their block matrix elements are of the form:

$$\langle f_p | \mathbb{GV}_k f_q \rangle = \alpha_q \int d^3 \mathbf{x} d^3 \mathbf{x}' f_p(\mathbf{x}) \mathbb{G}(\mathbf{x}, \mathbf{x}') f_q(\mathbf{x}')$$
 (8)

(see supplement for more details). The equivalence of (1) and (7) captures the seamless unification of ideas and methods previously confined to either atomistic vdW or continuum Casimir physics [40]: (7) is similar to prior log-determinant expressions used to describe molecular interactions in vacuum [8], except that  $\mathbb{G}_0$  and  $\mathbb{G}_{\mathrm{env}}$  are replaced by nonretarded (quasistatic) vacuum fields  $\mathbb{G}_0(\mathrm{i}\xi=0)$ .

We demonstrate the importance of all of these effects by comparing the vdW energies (or forces) obtained from (7) to those from pairwise or other approximate treatments in a number of configurations, consisting of one or two molecules above either a gold half-space or a conical gold tip. While the Green's function of the half-plate can be computed analytically [41], the latter is computed using brute-force numerical techniques [1, 26–28], with the dielectric function of gold taken from [16]. We specifically study a  $C_{500}$ -fullerene of radius 1 nm, a 250 atom 30 nm-long linear carbyne wire, and a 1944 atom-large 2.6 nm  $\times$  2.9 nm  $\times$  5.5 nm protein associated with human Huntington's disease [42–44].

We further compare the RMB energy from (7) to typical approximations used in the literature: the non-retarded vdW energy  $\mathcal{E}_0$ , obtained by evaluating (7) with  $\mathbb{G}_0$  and  $\mathbb{G}_{\mathrm{env}}$  replaced by their respective quasistatic (i $\xi=0$ ) responses, and the Casimir–Polder (CP) energy,

$$\mathcal{E}_{\mathrm{CP}} = -\frac{\hbar}{2\pi} \int_0^\infty d\xi \, \mathrm{Tr} \, \left[ \alpha \cdot \mathbb{G}_{\mathrm{env}} \cdot \left( \mathbb{I} + \frac{1}{2} \alpha \cdot \mathbb{G}_{\mathrm{env}} \right) \right]_{(9)}$$

which ignores finite size effects by instead contracting the dressed susceptibility of the molecular ensemble into effective dipolar polarizabilities,

$$\alpha = \bigoplus_{k} \sum_{p,q} \langle f_p | (\mathbb{I} - \mathbb{V}_k \mathbb{G}_0)^{-1} \mathbb{V}_k f_q \rangle,$$

thus neglecting higher-order many-body interactions among the different molecules and surfaces. Finally, we define a pairwise interaction energy,

$$\mathcal{E}_{\text{PWS}} = -\frac{\hbar}{2\pi} \int_0^\infty d\xi \operatorname{Tr} \left[ \sum_k \mathbb{V}_k \mathbb{G}_{\text{env}} \left( \mathbb{I} + \frac{1}{2} \sum_{l \neq k} \mathbb{V}_l \mathbb{G}_{\text{env}} \right) \right]$$
(10)

which, as in (9), is obtained as a lowest-order expansion of (7) in the scattering; this captures both finite size and retardation but ignores all high-order many-body interactions, with the sums over k, l running over either individual or pairs of molecules. When comparing non-retarded and CP energies to their corresponding pairwise approximations, it suffices to take the quasistatic limit in (10) and to let  $(\mathbb{I} - \mathbb{V}_k \mathbb{G}_0)^{-1} \to \mathbb{I}$  for the effective polarizability  $\alpha$  in (9), respectively.

Figure 2 shows the RMB to pairwise energy ratio  $\frac{\mathcal{E}}{\mathcal{E}_{\mathrm{PWS}}}$  of various configurations (insets), with the fullerene interaction (blue line) found to vary only slightly, attaining a maximum of 1.16 at  $z\approx 10$  nm; such a small discrepancy stems from the small size and isotropic shape of the fullerene, which limits possible nonlocal correlations in its polarization response. Even weaker relative correlations are observed in the case of the protein (green line), which despite its greater size, number of atoms, and chemical complexity, has a reduced response compared to semi-metallic carbon allotropes [8, 9]. To separate the various many-body effects, the inset of Fig. 2 compares the RMB power law  $\frac{\partial \ln(\mathcal{E})}{\partial \ln(z)}$  of the fullerene interaction to its counterparts when neglecting either finite size or retardation. As expected, both approximations become accurate

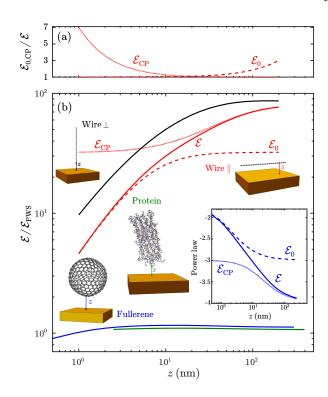


Figure 2. (a) CP  $\mathcal{E}_{\mathrm{CP}}$  (dotted red) and non-retarded  $\mathcal{E}_0$  (dashed red) energies of a parallel carbyne wire separated from a gold plate by a vertical distance z, normalized to the corresponding retarded, manybody energy  $\mathcal{E}$  of (7), as a function of z; (b) Energy ratio  $\frac{\mathcal{E}}{\mathcal{E}_{\mathrm{PWS}}}$  versus z for a range of molecules, i.e. a fullerene (solid blue), protein (solid green), or wire in the parallel (solid red) or perpendicular (solid black) orientations, above the gold plate;  $\mathcal{E}_{\mathrm{PWS}}$  is the energy obtained by a pairwise approximation defined in (10). Also shown are the predictions of both CP (dotted red) and non-retarded (dashed red) approximations for the case of a parallel wire. Inset: the power law  $\frac{\partial \ln(\mathcal{E})}{\partial \ln(z)}$  (solid blue) of the fullerene—plate system with respect to z, compared to both CP and non-retarded approximations.

in their corresponding regimes of validity, with the power law asymptoting to -4 and -1.9 at large and small z, respectively, but fail in the intermediate, mesoscopic regime  $z \approx 10 \text{ nm}$ . Even larger discrepancies arise in the case of the wire, whose large size and highly anisotropic shape support long-wavelength collective fluctuations. We find that the absolute values of both  $\mathcal{E}_0$  (dashed red) and  $\mathcal{E}_{\mathrm{CP}}$  (dotted red) for the parallel wire overestimate  $\mathcal{E}$  by factors of 3–7 [Fig. 2(a)] due to the slower decay of the Green's function in the former and lack of screening over the length (or modes) of the wire in the latter. The corresponding energy ratios, however, behave differently in that the effect of screening is strongest in the quasistatic limit, which ends up greatly dampening the many-body excitations relative to pairwise approximations and hence leads to smaller non-retarded energy ratios; in contrast, by construction CP ignores many-body interactions with the surface and thus screening has a much weaker impact relative to the pairwise approximation, leading to larger CP energy ratios. At intermediate  $z \approx 10 \text{ nm}$  of the order of the wire length,  $\mathcal{E}/\mathcal{E}_{PWS} \approx 30$ , with the approximate energy ra-

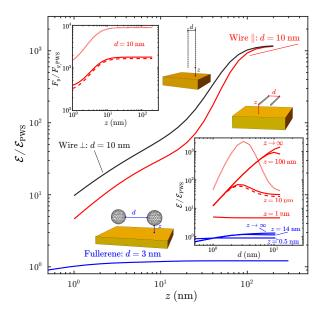


Figure 3. Energy ratio  $\frac{\mathcal{E}}{\mathcal{E}_{\mathrm{PWS}}}$  versus vertical distance z for two fullerenes at fixed horizontal separation d=3 nm (solid blue) or two wires at d=10 nm, in either the parallel (solid red) or perpendicular (solid black) orientations, above a gold plate. Top inset: horizontal-force ratio  $\frac{F_y}{F_{y,\mathrm{PWS}}}$  versus z for the parallel wires at d=10 nm. Bottom inset:  $\frac{\mathcal{E}}{F_{y,\mathrm{PWS}}}$  versus d for the fullerenes and the parallel wires at several values of z; also shown are the corresponding ratios obtained via CP (dotted red) and non-retarded (dashed red) approximations, for the particular case of z=10 nm.

tios deviating by 20%. Similar results are observed in the case of a wire in the perpendicular orientation (black lines), with the pairwise energy leading to slightly larger discrepancies at short separations due to the screening and decreasing impact of atoms farther away from the plate.

We now investigate the mutual vdW interactions among two fullerenes or parallel wires oriented either parallel or perpendicular to the gold plate [Fig. 3], focusing primarily on horizontal separations d on the order of molecular sizes, where many-body and finite size effects are strongest. Especially in the case of two wires, the pairwise approximation is shown to fail by many orders of magnitude, with the largest energy ratios occurring at asymptotically large z, i.e. for two molecules in vacuum, while at small z a decreasing ratio reflects the dominant interactions (and screening) of the individual molecules with the plate. The transition and competition between the two limiting behaviors occurs at mesoscopic  $z \sim d$ , and is more clearly visible from the plots in Fig. 3(lower inset), which show  $\frac{\mathcal{E}}{\mathcal{E}_{\mathrm{PWS}}}$  versus d at several values of z. In particular, in the case of parallel wires at mesoscopic z = 10 nm, the competition leads to a nonmonotonic energy ratio, with the maximum of 70 occurring at intermediate  $d \approx 3$  nm. Comparisons against non-retarded and CP approximations illustrate behaviors similar to the previous case of a single wire, with each under- and over-estimating the ratios by approximately 20% and 30%, respectively. Also

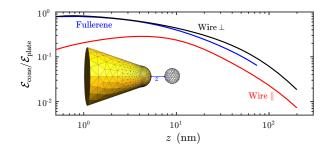


Figure 4. Energy  $\mathcal{E}_{\mathrm{cone}}$  of either a fullerene (solid blue) or carbyne wire (solid red/black) above a gold cone, normalized to the energy  $\mathcal{E}_{\mathrm{plate}}$  of the same molecule but separated from a gold plate by the same surface–surface vertical distance z.

shown in Fig. 3(upper inset) is the ratio of the horizontal force  $F_y=-\frac{\partial \mathcal{E}}{\partial y}$  on the wires to its pairwise counterpart, plotted against z for parallel wires at d=10 nm. Note that by construction,  $F_{y,\mathrm{PWS}}$  is independent of z and thus, the system experiences an absolute decrease in the force due to the screening induced by the plate. Comparing  $F_{y,0}$  and  $F_{y,\mathrm{CP}}$ , one finds the surprising result that in contrast to the energy ratio of a single molecule, the screening by the plate makes retardation more rather than less relevant to the force at small z, leading to an  $\approx 10\%$  decrease in the force magnitude.

Finally, we consider the energy of a molecule above a gold conical tip [Fig. 4] by comparing it to that of a gold plate at the same vertical separation z, with  $\mathbb{G}_{env}$  in the former computed through the use of a free, surface-integral Maxwell solver, SCUFF-EM [45, 46]. The finite cone has a base diameter of 54 nm and a height of 50 nm from the base to the bottom of a hemispherical tip of diameter 20 nm. The ratio decreases with increasing z, with the energy scaling as  $z^{-6}$  at asymptotically large separations (not shown) as the finite sizes of the cone and molecule become irrelevant and their interactions dipolar. (Note that a decreasing ratio is expected also for a semi-infinite cone due to its smaller effective area and hence stronger decay compared to a plate.) The ratios at small z for the fullerene and perpendicular wire approach 1 since in this limit, their small horizontal sizes allow the hemispherical tip, which effectively acts like a plate at such short separations, to dominate the interaction. By contrast, the ratio in the case of a parallel wire is non-monotonic, decreasing with at short separations since in this configuration, the wire excitations in the limit  $z \to 0$  still sample the finite curvature of the tip and conical slope, leading to a different asymptotic power law.

In conclusion, we have demonstrated a unifying approach to computing vdW interactions among molecules and macroscopic bodies that accounts for many-body and multiple-scattering effects to all orders. By comparing against commonplace pairwise, CP, and non-retarded approximations, we quantified the impact of nonlocality, finite size, and retardation on the vdW energy between molecules and either a planar or conical macroscopic body. We have consistently found larger deviations in approximate interactions for long, semi-metallic molecules such as carbyne wires, whereas compact,

insulating molecules such as many proteins are reasonably well-described as effectively dilute dielectric particles, allowing these low-order approximations to be more valid. In the future, one might consider more complex macroscopic bodies, such as periodic gratings [17, 18] that may elicit larger differences between RMB and approximate interactions even for compact biomolecules, as well as extend these results to incorporate the effects of infrared molecular resonances [16].

This material is based upon work supported by the National Science Foundation under Grant No. DMR-1454836 and by the National Science Foundation Graduate Research Fellowship Program under Grant No. DGE 1148900.

## Appendix A: Approximations

Our calculations above make two related approximations related to Gaussian damping. First, we approximate (8) as

$$\langle f_p | \mathbb{GV}_k f_q \rangle \approx \alpha_q \int d^3 \mathbf{x}' \, \mathbb{G}(i\xi, \mathbf{x}_p, \mathbf{x}') f_{p+q}(i\xi, \mathbf{x}') \quad (A1)$$

where  $f_{p+q}$  is the same as  $f_q$ , but with  $\sqrt{2}\sigma_p$  replaced with  $\sqrt{\sigma_p^2 + \sigma_q^2}$ , in line with [8]; this effectively approximates the Galerkin discretization by a collocation method, with the basis Gaussian functions  $f_{p+q}$  acquiring modified widths. Secondly, for computational convenience, we consider only scattered fields (Green's functions) from dipolar rather than Gaussian sources, which is justified so long as the atoms are several widths (angstroms) away from the macroscopic surfaces.

## Appendix B: vdW energy via fluctuation-dissipation theorem

We provide a heuristic derivation of the retarded, many-body (RMB) vdW energy of a general collection of molecular or macroscopic bodies, requiring only that they be disjoint and have no correlations in the polarization response between bodies. Each body k is described by an electric susceptibility  $\mathbb{V}_k$ , relating its polarization to the total electric field via  $|\mathbf{P}_k\rangle = \mathbb{V}_k|\mathbf{E}\rangle$ ; these susceptibilities account for short-range quantum and electrostatic correlations, allowing us to focus solely on long-range electrodynamic correlations when considering the vdW energy. [47] Our derivation follows analysis [48–50] based on the fluctuation—dissipation theorem; we note previous demonstrations [6, 51] of its equivalence to the summation of ground-state energies of the coupled molecular system [34, 52].

Following Ref. 48, the assembly of the constituents of all bodies from infinite separation into the final configuration defining  $\mathbb{V} = \sum_k \mathbb{V}_k$  can be considered the result of an adiabatic change in the particle–field coupling strength  $\lambda \in [0,1]$ , in which case the energy of the system can be written as,

$$\mathcal{E} = -\int_0^\infty d\omega \int_0^1 \frac{d\lambda}{\lambda} \langle \langle \mathbf{P} | \mathbf{E} \rangle \rangle_{\text{ZP}}, \tag{B1}$$

per the Feynman–Hellmann theorem [48, 49]. Here,  $|\mathbf{E}\rangle$  denotes zero-point fluctuating electric fields,  $|\mathbf{P}\rangle = \mathbb{V}|\mathbf{E}\rangle$  is the induced polarization, and  $\langle \rangle_{\mathrm{ZP}}$  denotes the quantum statistical average over zero-point fluctuations. The connection to scattering problems comes from the well-known fluctuation–dissipation theorem [26],

$$\langle |\mathbf{E}\rangle \langle \mathbf{E}| \rangle_{\mathrm{ZP}} = \frac{\hbar}{\pi} \mathrm{Im} \, \mathbb{G},$$
 (B2)

which expresses field fluctuations in terms of the Green's function  $\mathbb{G}$  of the system. The latter solves Maxwell's equations and can be written in terms of the susceptibility as  $\mathbb{G} = (\mathbb{I} - \mathbb{G}_0 \mathbb{V})^{-1} \mathbb{G}_0$  [29]. Exploiting the analyticity of  $\mathbb{V}$  and  $\mathbb{G}_0$  in the complex- $\omega$  plane [28, 37] and performing a Wick rotation of the energy integral from real to imaginary frequency  $\omega = i\xi$ , leads to a simplified expression for the energy [53],

$$\mathcal{E} = \frac{\hbar}{2\pi} \int_0^\infty d\xi \ln\left(\det\left(\mathbb{I} - \mathbb{G}_0\mathbb{V}\right)\right)$$
 (B3)

where we rescaled the response functions  $\mathbb{G}_0$  and  $\mathbb{V}$  by the coupling constant  $\lambda$  and integrated over  $\lambda$ . The net interaction energy among the bodies is found by subtracting self-energies of the form in (B3), replacing  $\mathbb{V}$  by  $\mathbb{V}_k$  separately for each k. This allows recasting the net vdW interaction energy as (7) in terms of scattering operators:

$$\mathbb{M} = \mathbb{I} - \mathbb{G}_0 \mathbb{V} \tag{B4}$$

$$\mathbb{M}_{\infty} = \prod_{k} (\mathbb{I} - \mathbb{G}_0 \mathbb{V}_k). \tag{B5}$$

If the system considered consists of N molecular bodies labeled k, and an arbitrary number of macroscopic bodies collectively described by  $\mathbb{V}_{\text{env}}$ , then one can write

$$\mathbb{M} = \mathbb{I} - \mathbb{G}_0 \mathbb{V}_{\text{env}} - \mathbb{G}_0 \mathbb{V} \tag{B6}$$

$$\mathbb{M}_{\infty} = (\mathbb{I} - \mathbb{G}_0 \mathbb{V}_{\text{env}}) \prod_k (\mathbb{I} - \mathbb{G}_0 \mathbb{V}_k), \tag{B7}$$

where  $\mathbb{V}=\sum_k \mathbb{V}_k$  only runs over the molecular bodies. Multiplying  $\mathbb{MM}_{-}^{-1}$  produces terms of the form

$$(\mathbb{I} - \mathbb{G}_0 \mathbb{V}_{\text{env}})^{-1} \mathbb{G}_0 \equiv \mathbb{G}_{\text{env}}, \tag{B8}$$

which is just the electric field response due to  $\mathbb{V}_{\mathrm{env}}$  alone and can be computed via analytical or numerical formulations of continuum electrodynamics. Redefining

$$\mathbb{M}' = \mathbb{I} - \mathbb{G}_{env} \mathbb{V} \tag{B9}$$

$$\mathbb{M}'_{\infty} = \prod_{k} (\mathbb{I} - \mathbb{G}_0 \mathbb{V}_k), \tag{B10}$$

and dropping primes, these new operators can then be substituted into (7) to obtain the net vdW interaction energy among N molecules and a general macroscopic environment.

[1] L. M. Woods, D. A. R. Dalvit, A. Tkatchenko, P. Rodriguez-Lopez, A. W. Rodriguez, and R. Podgornik, Rev. Mod. Phys. 88, 045003 (2016).

- [2] D. Langbein, "Theory of van der waals attraction," in *Springer Tracts in Modern Physics* (Springer Berlin Heidelberg, Berlin, Heidelberg, 1974) pp. 1–139.
- [3] A. Tkatchenko, Advanced Functional Materials 25 (2015).
- [4] A. D. McLachlan, Molecular Physics **6**, 423 (1963).
- [5] M. W. Cole, D. Velegol, H.-Y. Kim, and A. A. Lucas, Molecular Simulation 35, 849 (2009).
- [6] A. Tkatchenko, A. Ambrosetti, and R. A. DiStasio Jr., The Journal of Chemical Physics 138 (2013).
- [7] V. V. Gobre and A. Tkatchenko, Nature Communications 4 (2013).
- [8] R. A. DiStasio Jr., V. V. Gobre, and A. Tkatchenko, Journal of Physics: Condensed Matter 26, 213202 (2014).
- [9] A. Ambrosetti, N. Ferri, R. A. DiStasio, Jr., and A. Tkatchenko, Science 351, 1171 (2016).
- [10] A. D. Phan, L. M. Woods, and T.-L. Phan, Journal of Applied Physics 114 (2013).
- [11] A. M. Reilly and A. Tkatchenko, Chem. Sci. 6, 3289 (2015).
- [12] Y. V. Shtogun and L. M. Woods, The Journal of Physical Chemistry Letters 1, 1356 (2010).
- [13] A. Ambrosetti, A. M. Reilly, R. A. DiStasio, and A. Tkatchenko, The Journal of Chemical Physics 140 (2014).
- [14] H.-Y. Kim, J. O. Sofo, D. Velegol, M. W. Cole, and A. A. Lucas, Langmuir 23, 1735 (2007).
- [15] A. Tkatchenko, R. A. DiStasio Jr., R. Car, and M. Scheffler, Phys. Rev. Lett. 108, 236402 (2012).
- [16] S. Y. Buhmann, S. Scheel, S. A. Ellingsen, K. Hornberger, and A. Jacob, Phys. Rev. A 85, 042513 (2012).
- [17] S. Y. Buhmann, V. N. Marachevsky, and S. Scheel, International Journal of Modern Physics A 31, 1641029 (2016).
- [18] H. Bender, C. Stehle, C. Zimmermann, S. Slama, J. Fiedler, S. Scheel, S. Y. Buhmann, and V. N. Marachevsky, Phys. Rev. X 4, 011029 (2014).
- [19] P. Thiyam, C. Persson, B. E. Sernelius, D. F. Parsons, A. Malthe-Sørenssen, and M. Boström, Phys. Rev. E 90, 032122 (2014).
- [20] P. Barcellona, R. Passante, L. Rizzuto, and S. Y. Buhmann, Phys. Rev. A 93, 032508 (2016).
- [21] F. Intravaia, C. Henkel, and M. Antezza, "Fluctuation-induced forces between atoms and surfaces: The casimir–polder interaction," in *Casimir Physics*, edited by D. Dalvit, P. Milonni, D. Roberts, and F. da Rosa (Springer Berlin Heidelberg, Berlin, Heidelberg, 2011) pp. 345–391.
- [22] M. DeKieviet, U. D. Jentschura, and G. Łach, "Modern experiments on atom-surface casimir physics," in *Casimir Physics*, edited by D. Dalvit, P. Milonni, D. Roberts, and F. da Rosa (Springer Berlin Heidelberg, Berlin, Heidelberg, 2011) pp. 393–418.
- [23] J. F. Babb, Journal of Physics: Conference Series 19, 1.
- [24] S. Y. Buhmann, Dispersion Forces I: Macroscopic Quantum Electrodynamics and Ground-State Casimir, Casimir–Polder and van der Waals Forces (Springer Berlin Heidelberg, Berlin, Heidelberg, 2012).
- [25] S. Y. Buhmann, Dispersion Forces II: Many-Body Effects, Excited Atoms, Finite Temperature and Quantum Friction (Springer Berlin Heidelberg, Berlin, Heidelberg, 2012).
- [26] S. G. Johnson, "Numerical methods for computing casimir interactions," in *Casimir Physics*, edited by D. Dalvit, P. Milonni, D. Roberts, and F. da Rosa (Springer Berlin Heidelberg, Berlin, Heidelberg, 2011) pp. 175–218.

- [27] A. W. Rodriguez, P.-C. Hui, D. P. Woolf, S. G. Johnson, M. Lončar, and F. Capasso, Annalen der Physik 527, 45 (2015).
- [28] A. W. Rodriguez, F. Capasso, and S. G. Johnson, Nature Photonics 5, 211 (2011).
- [29] S. J. Rahi, T. Emig, N. Graham, R. L. Jaffe, and M. Kardar, Phys. Rev. D 80, 085021 (2009).
- [30] M. T. H. Reid, J. White, and S. G. Johnson, Phys. Rev. A 88, 022514 (2013).
- [31] X. Ge and D. Lu, Phys. Rev. B 92, 241107 (2015).
- [32] A. G. Donchev, The Journal of Chemical Physics 125 (2006).
- [33] J. Mahanty and B. W. Ninham, J. Chem. Soc., Faraday Trans. 2 71, 119 (1975).
- [34] M. J. Renne, Physica 53, 193 (1971).
- [35] A. Mayer, Phys. Rev. B 75, 045407 (2007).
- [36] A. Lambrecht, P. A. M. Neto, and S. Reynaud, New Journal of Physics 8, 243 (2006).
- [37] A. Rodriguez, M. Ibanescu, D. Iannuzzi, J. D. Joannopoulos, and S. G. Johnson, Phys. Rev. A 76, 032106 (2007).
- [38] A. W. Rodriguez, A. P. McCauley, J. D. Joannopoulos, and S. G. Johnson, Phys. Rev. A **80**, 012115 (2009).
- [39] A. P. McCauley, A. W. Rodriguez, J. D. Joannopoulos, and S. G. Johnson, Phys. Rev. A 81, 012119 (2010).
- [40] R. H. French, V. A. Parsegian, R. Podgornik, R. F. Rajter, A. Jagota, J. Luo, D. Asthagiri, M. K. Chaudhury, Y.-m. Chiang, S. Granick, S. Kalinin, M. Kardar, R. Kjellander, D. C. Langreth, J. Lewis, S. Lustig, D. Wesolowski, J. S. Wettlaufer, W.-Y. Ching, M. Finnis, F. Houlihan, O. A. von Lilienfeld, C. J. van Oss, and T. Zemb, Rev. Mod. Phys. 82, 1887 (2010).
- [41] in *Principles of Nano-Optics* (Cambridge University Press, 2006) pp. 335–362.
- [42] N. Ferguson, J. Becker, H. Tidow, S. Tremmel, T. D. Sharpe, G. Krause, J. Flinders, M. Petrovich, J. Berriman, H. Oschkinat, and A. R. Fersht, 103, 16248 (2006).
- [43] H. M. Berman, J. Westbrook, Z. Feng, G. Gilliland, T. N. Bhat, H. Weissig, I. N. Shindyalov, and P. E. Bourne, 28, 235 (2000).
- [44] H. Berman, K. Henrick, and H. Nakamura, Nat Struct Mol Biol 10, 980 (2003).
- [45] M. T. H. Reid and S. G. Johnson, IEEE Transactions on Antennas and Propagation 63, 3588 (2015).
- [46] http://homerreid.com/scuff-EM.
- [47] When neglecting retardation, the *charge* density and electric potential are more frequently used, so the density response is written in terms of the susceptibility as  $\chi(\omega, \mathbf{x}, \mathbf{x}') = \sum_{i,j} \partial_i \partial_j(\mathbb{V}_k)_{ij}(\omega, \mathbf{x}, \mathbf{x}')$ .
- [48] F. S. S. Rosa, D. A. R. Dalvit, and P. W. Milonni, Phys. Rev. A 84, 053813 (2011).
- [49] G. S. Agarwal, Phys. Rev. A 11, 243 (1975).
- [50] T. B. MacRury and B. Linder, The Journal of Chemical Physics 58, 5388 (1973).
- [51] J. Mahanty and B. W. Ninham, Journal of Physics A: General Physics 5, 1447.
- [52] M. J. Renne, Physica 56, 125 (1971).
- [53] The entirety of this derivation is identical to that of past work employing the so-called adiabatic connection fluctuation dissipation (ACFD) framework, but using the vector polarization, tensor electric susceptibility, and tensorial vacuum Green's function instead of the scalar charge density, density response, or Coulomb potential, in order to account for retardation. It is therefore not a coincidence that the log-determinant frequency integrand is so similar in form to past expressions for the vdW energy of a single body.